

# Possible Sources of Imaging Performance Degradation in Advanced Spaceborne SAR Systems Based on Scan-On-Receive

Federica Bordoni  
Microwaves and Radar Institute  
German Aerospace Center (DLR)  
Oberpfaffenhofen, Germany  
federica.bordoni@dlr.de

Marc Rodriguez-Cassola  
Microwaves and Radar Institute  
German Aerospace Center (DLR)  
Oberpfaffenhofen, Germany  
marc.rodriguez@dlr.de

Gerhard Krieger  
Microwaves and Radar Institute  
German Aerospace Center (DLR)  
Oberpfaffenhofen, Germany  
gerhard.krieger@dlr.de

**Abstract**—The scan-on-receive capability is a fundamental feature of advanced spaceborne synthetic aperture radar (SAR) systems for high-resolution wide-swath imaging. The achievable SAR imaging performance depends on the possibility to properly collect the backscattered energy of interest, and to effectively suppress undesired returns. Nevertheless, the related signal model, reported in the literature, does not reflect the complexity of a real acquisition scenario. This paper identifies possible sources of image quality degradation, generally neglected, specific of this kind of systems. It provides a first analysis of their effect in dependence of instrument and acquisition geometry parameters, as support for tasks of system design and image quality assessment.

**Keywords**—synthetic aperture radar, digital beamforming, scan-on-receive.

## I. INTRODUCTION

Future high-resolution wide-swath synthetic aperture radar (SAR) systems will be able to deliver images with overall improved quality if compared to the present systems [1]–[11]. Their fundamental characteristic is the use of multiple digital channels in combination with innovative digital beamforming (DBF) techniques [3], [4]. Outstanding among these techniques is the scan-on-receive (SCORE) [1], included in advanced missions, such as the United States-Indian NISAR, the European Sentinel-1 Next Generation, and the German Tandem-L [6], [9], [10].

According to SCORE, a large swath is illuminated by using a wide transmit (Tx) beam; whereas on reception (Rx), a sharp and high gain beam scans the illuminated swath from near to far range, following the pulse echo as it travels along the ground range direction [1]. Such a use of a sharp and high gain Rx beam, with respect to a conventional approach based on a wide and static beam, allows for improved radiometric performance all over the swath, as well as a more efficient suppression of range ambiguous signals.

The mentioned, original SCORE approach was extended by more advanced elevation DBF concepts. Here, an ultra-wide swath is illuminated by using a pulse repetition interval (PRI) shorter than the receiving window [9], [10], or multiple subpulses are transmitted within the same PRI [3], [11], [12]. Then, on Rx, multiple beams are used to collect the echoes simultaneously arriving from different directions of arrival (DoA) within the imaged swath. Further advanced extensions of SCORE concept consider the incorporation in the

elevation DBF of null-steering techniques, to improve the suppression of the undesired returns [3], [5].

A full exploitation of the advantages offered by SCORE-based systems is constrained by the knowledge of the DoA of the Rx signals, useful and ambiguous. This is a prerequisite to properly collect the backscattered energy of interest, and to effectively suppress undesired returns. Nevertheless, according to the literature, the computation of the Rx signal DoA is based on simple models, that neglect the complexity of a real acquisition scenario [1], [5]. As an example, the actual terrain morphology, as well as deviations from the vertical zero Doppler plane geometry, are not considered. It is worth to remark that these simple models are applied also for the evaluation of the achievable SAR imaging performance.

This paper provides a first analysis of the impact of a real acquisition scenario on SCORE performance, as support for system design and image quality assessment of advanced DBF SAR systems.

## II. SCORE PATTERN AND RECEIVED POWER

In order to explain the importance of a proper identification of the DoA of the Rx signals in SCORE-based systems, it is useful to consider the expression of the signal-to-noise ratio (SNR) of a resolution cell<sup>1</sup>, and in particular the contribution of the SCORE Rx pattern. For simplicity, let us refer to a planar array antenna and a stripmap operational mode. The SNR as a function of the slant range is generally computed as:

$$SNR(R) \approx const \frac{\sigma |P_{el}^{TX} P_{el}^{RX}|^2}{\sin(\vartheta_{inc}) R^3}, \quad (1)$$

$R$  denoting the slant range,  $\sigma$  the backscattering coefficient,  $\vartheta_{inc}$  the incidence angle,  $P_{el}^{RX}$  and  $P_{el}^{TX}$  the Rx and Tx elevation pattern values, corresponding with the resolution cell of interest<sup>2</sup>;  $const$  a factor, constant over the swath.

Eq. (1) is used also for conventional systems [13]. The peculiarity of SCORE-based systems is that the pointing

<sup>1</sup> The relevant SAR imaging performance parameters, noise equivalent sigma zero (NESZ) and range ambiguity-to-signal ratio (RASR), are strictly related with the SNR [13].

<sup>2</sup> The geometrical relationships are computed with reference to the zero Doppler plane crossing the resolution cell.

direction of  $P_{el}^{RX}$  varies with the slant range, so that the related array factor is maximum for each  $R$ .

Indeed, the SNR in eq. (1) is obtained under the following assumptions: (i) SCORE Rx elevation pattern value,  $P_{el}^{RX}$ , is constant during the azimuth illumination time; (ii) each sample from a resolution cell, within a sweep, is weighted by the same value of  $P_{el}^{RX}$ ; (iii) this constant value of  $P_{el}^{RX}$  is the maximum one, i.e. SCORE steering direction always corresponds with the DoA of the echo received from the resolution cell. Nevertheless, in a real scenario, a pointing error and consequently a loss may occur.

For a given SCORE mispointing, the entity of the loss depends on the shape of the Rx beam: the sharper the beam, the higher the loss. In order to identify relevant values of pointing errors, Fig. 1 shows the mispointing associated with a SCORE pattern loss<sup>3</sup> (SPL) of about -0.3 dB, for a rectangular antenna of variable height and different radar wavelengths. Note that typical requirements on the radiometric accuracy and stability are in the order of 0.5 dB.

The considerations reported so far regard the power received from the signal of interest. Nevertheless, they can be easily extended to the power received from a range ambiguous signal. In this case, the mispointing can produce a very strong variation on the received power, depending on the location of the ambiguous source. Particularly critical is the case of an ambiguous signal located in proximity of a null of the Rx pattern. Nevertheless, if null-steering is not applied to suppress the ambiguities, the effect of a mispointing on the range ambiguity-to-signal ratio (RASR) is mitigated by the number of ambiguities and by the migration of the ambiguous sources with the pulse propagation.

### III. SOURCES OF LOSSES

This section identifies possible sources of SCORE mispointing, and provides a first analysis of their individual effect. The following formulation of SCORE is considered [1]: the steering direction of SCORE Rx pattern varies as a function of the range time; it is given by the instantaneous DoA of the center of the backscattered pulse of interest, computed in the zero Doppler plane under the assumption of a pure spherical Earth model (i.e. variations in the terrain elevation are not accounted for). Additionally, except for Subsection III.B, a negligible pulse duration is assumed.

#### A. Topographic Variations

Let us consider the vertical, zero Doppler, plane: the DoA of a point target with terrain height  $\Delta h$  differs from that of an isorange target with no elevation. The resulting SCORE mispointing can be expressed as [3], [14]:

$$\Delta\theta_h \approx \frac{\Delta h}{R \sin(\vartheta_{inc})}, \quad (2)$$

$R$  and  $\vartheta_{inc}$  denoting the slant range and the incidence angle at SCORE pointing direction.

<sup>3</sup> The SPL is defined as the value of the SCORE elevation Rx gain pattern in the actual DOA of the signal, normalized to its maximum value.

Fig. 2 shows  $\Delta\theta_h$  versus incidence angle, for  $\Delta h$  values between 500 m and 2000 m, and an orbit height of 500 km. The worst value is achieved in near range: here, for an incidence angle of 20 deg,  $\Delta\theta_h$  varies between about 0.15 and 0.6 deg. For ambiguous signals, located in near range, the mismatch is even larger.  $\Delta\theta_h$  decreases for higher orbit height values.

It is worth to note that, in a realistic acquisition scenario, SCORE steering can be adapted only partially to the actual terrain morphology. In fact, inherent limitations occur when it is not possible to define a single instantaneous DoA, due to fast topographic variations in the elevation direction (layover) or in the azimuth direction within the antenna beam footprint [7], [14].

#### B. Pulse Duration

The echo from a point target lasts for a time interval, given by the duration of the Tx pulse,  $\tau_p$ . During this interval, the DoA of the backscattered signal is constant, but SCORE Rx beam moves. Specifically, for a target of interest, the pointing direction variation is:

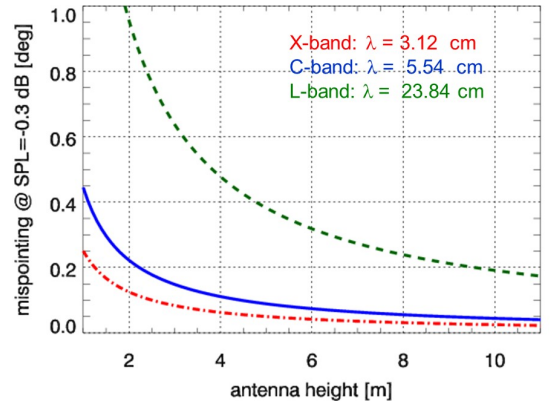


Fig. 1. Absolute value of the pointing error corresponding to a SPL of about -0.3 dB, versus height of a uniformly weighted rectangular aperture, for different radar wavelengths.

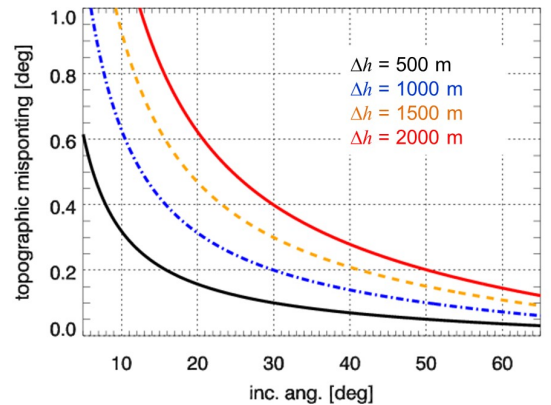


Fig. 2. Mispointing due to unexpected terrain elevation,  $\Delta h$ , versus incidence angle. Orbit height: 500 km.

$$\Delta\theta_s = \theta_s \left( t_0 + \frac{\tau_p}{2} \right) - \theta_s \left( t_0 - \frac{\tau_p}{2} \right), \quad (3)$$

being  $t_0$  the instant when SCORE beam is steered toward the target. Accordingly, without a proper compensation, the backscattered echo is weighted by the SCORE Rx pattern sector corresponding with  $\Delta\theta_s$ . It is worth noting that  $\Delta\theta_s$  depends not only on the pulse duration, but also on the Rx beam steering velocity, i.e. on SCORE steering law<sup>4</sup>.

Fig. 3 shows  $\Delta\theta_s$  versus incidence angle, for different orbit height values, a pulse duration of 48  $\mu$ s, and a SCORE steering law based on a pure spherical Earth model [15].

The previous considerations can be easily extended to the range ambiguous echoes. Fig. 4 shows an example of pattern sectors, weighting signal of interest (green) and ambiguities (red).

### C. Pulse Bandwidth

The antenna pattern shape depends on the operational frequency. In particular, for the elevation pattern of a planar array, steered by means of a constant phase excitation, the pointing and null directions are given respectively by:

$$\theta_{\max}(f) = \arcsin \left( \frac{\sin(\theta_0)}{1 + \frac{\Delta f}{f_0}} \right), \quad (4)$$

$$\theta_{\text{null}}(f) = \arcsin \left\{ \frac{n \frac{\lambda_0}{H_{\text{ant}}} + \sin(\theta_0)}{1 + \frac{\Delta f}{f_0}} \right\}, \quad (5)$$

where,  $H_{\text{ant}}$  is the antenna height;  $n = \pm 1, \pm 2, \dots$  the null number;  $\theta_0$  the nominal steering angle;  $f = f_0 + \Delta f$  the operational frequency;  $f_0$  the nominal frequency (the central frequency of the pulse);  $\lambda_0$  the nominal radar wavelength;  $\Delta f$  the frequency variation within the pulse bandwidth,  $B_c$ , i.e.  $-B_c/2 \leq \Delta f \leq B_c/2$ .

Since the chirp pulse is linear frequency modulated, each sample of the echo received from a point target is characterized by a different frequency. Accordingly, in absence of a proper compensation, the samples are weighted by patterns, different from the nominal one. Note, that this effect occurs even in case of short pulses, and depends through the pulse bandwidth,  $B_c$ , on the desired range resolution.

As an example, Fig. 5 shows the angular deviation from the nominal value of the pattern pointing and null direction, obtained for  $\Delta f = -B_c/2$ , in case of an L-band system with antenna height of 3.5 m and a chirp bandwidth of 88 MHz (ground range resolution below 5 m for incidence angles larger than 20 deg).

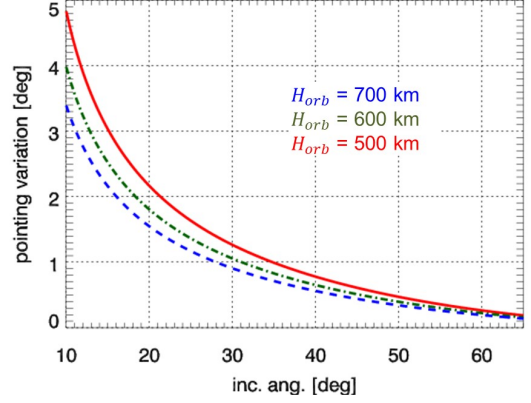


Fig. 3. Variation of SCORE pointing direction associated with a pulse duration of 48  $\mu$ s, versus incidence angle, for different orbit heights.

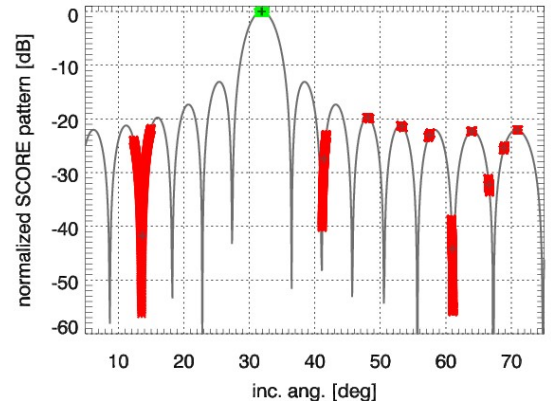


Fig. 4. Normalized SCORE Rx elevation gain pattern and pattern sectors for the useful signal (green) and the ambiguities (red). Pulse duration: 48  $\mu$ s; duty cycle: 8%; PRF: 1650 Hz; orbit height: 700 km; antenna height: 3.5 m; radar wavelength: 23.84 cm.

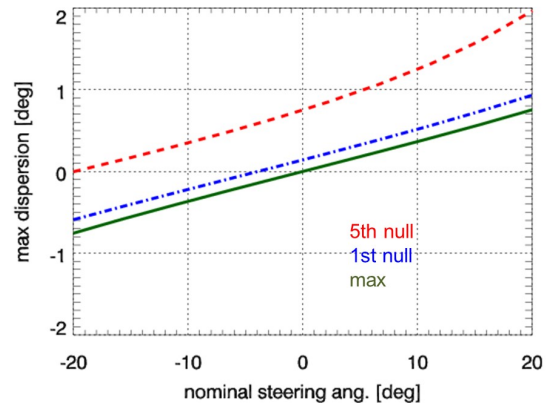


Fig. 5. Maximum angular deviation from the nominal value of the pointing and null direction, versus nominal steering angle. Antenna height: 3.5 m; radar wavelength: 23.84 cm; chirp bandwidth: 88 MHz; null number: 1, 5.

<sup>4</sup> A solution to compensate the loss induced by the pulse duration is suggested in [1], for a SCORE steering law based on a pure spherical Earth model, i.e. without considering variations in the terrain elevation.

#### D. Range Cell Migration

Let us consider a spherical Earth model: during the illumination time, the target slant range and DoA vary. In particular, the DoA of a target located outside the zero Doppler plane is different from that of a target in the zero Doppler plane with the same slant range (range time). Since the pointing direction of SCORE Rx pattern is computed based on the zero Doppler plane geometry, a mispointing occurs during the target exposure time. The resulting angular mismatch, associated with the range cell migration (RCM), can be written as:

$$\Delta\theta_{rcm} = \hat{\theta}_1 - \theta_s = \hat{\theta}_1 - \theta_0, \quad (6)$$

where  $\hat{\theta}_1$  denotes the DoA of the target during the exposure, expressed as equivalent antenna elevation angle;  $\theta_0$  the DoA of an isorange target in the zero Doppler plane;  $\theta_s$  SCORE steering direction.

The maximum of  $\Delta\theta_{rcm}$  is proportional to the azimuth beam size, i.e. depends on the radar wavelength and the desired azimuth resolution; it is independent on the orbit height. Fig. 6 shows, as an example, the maximum value of  $\Delta\theta_{rcm}$  for an L-band system and different resolution values.

#### IV. CONCLUSIONS

The imaging performance of advanced spaceborne SAR systems based on scan-on-receive (SCORE) depends on the possibility to properly retrieve the direction of arrival (DoA) of the received signals, useful and ambiguous. The paper identifies and analyses potential sources of performance degradation. A first analysis of their individual effect, also in dependence of instrument and acquisition geometry parameters, is provided. The obtained results show that the effect of terrain morphology, range cell migration, pulse duration and bandwidth, should be carefully considered in order to properly define the DoA of the received signals. Mutual effects and interactions deserve attention too.

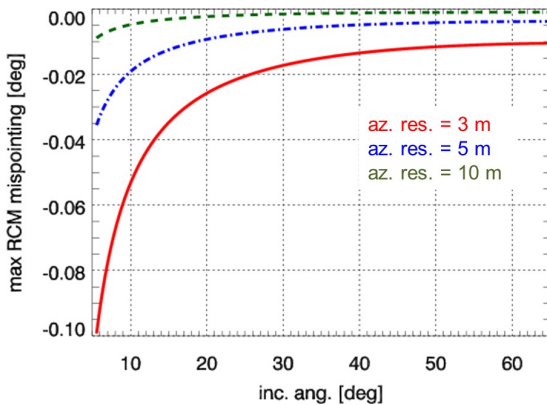


Fig. 6. Angular mismatch associated with the maximum RCM, versus incidence angle, for different azimuth resolution values and a radar wavelength of 23.84 cm.

Inherent limitations of the SCORE technique, especially in scenarios characterized by fast topographic variations, are also highlighted.

#### ACKNOWLEDGMENT

The authors thank their colleagues S. Huber and U. Steinbrecher for the useful discussions.

#### REFERENCES

- [1] M. Suess, B. Grafmueller, R. Zahn, "A Novel High Resolution, Wide Swath SAR System", in Pro. IGARSS, vol. 3, pp. 1013-1015, July 2001.
- [2] G. Krieger, N. Gebert, A. Moreira, "Unambiguous SAR signal reconstruction from nonuniform displaced phase center sampling", IEEE Tran. Geosci. and Remote Sen. Letters, vol. 1, no. 4, pp. 260 - 264, Oct. 2004.
- [3] G. Krieger, N. Gebert, A. Moreira, "Multidimensional Waveform Encoding: A New Digital Beamforming Technique for Synthetic Aperture Radar Remote Sensing", IEEE Tran. on Geosci. and Remote Sen., vol. 46, no. 1, pp.31-46, Jan. 2008.
- [4] N. Gebert, G. Krieger, and A. Moreira, "Digital Beamforming on Receive: Techniques and Optimization Strategies for High-Resolution Wide-Swath SAR Imaging", IEEE Tran. on Aero. and Electron. Sys., vol. 45, no. 2, pp. 564-592, April 2009.
- [5] F. Feng, S. Li, W. Yu, P. Huang, W. Xu, "Echo Separation in Multidimensional Waveform Encoding SAR Remote Sensing Using an Advanced Null-Steering Beamformer", IEEE Tran. on Geosci. and Remote Sen., vol. 50, no. 10, pp.4157-4172, Oct. 2012.
- [6] G. Adamiuk, C. Schaefer, C. Fischer, and C. Heer, "SAR Architectures Based on DBF for C- and X-Band Applications", Pro. EUSAR, June 2014.
- [7] G. Krieger, S. Huber, M. Villano, M. Younis, T. Rommel, P. Lopez Dekker, F. Queiroz de Almeida, A. Moreira, "CEBRAS: Cross Elevation Beam Range Ambiguity Suppression for High-Resolution Wide-Swath and MIMO-SAR Imaging", Pro. IGARSS, pp. 196-199, July 2015.
- [8] G. Krieger, S. Huber, M. Villano, F. Queiroz de Almeida, M. Younis, F. López Dekker, P. Prats, M. Rodriguez Cassola, A. Moreira, "SIMO and MIMO System Architectures and Modes for High-Resolution Ultra-Wide-Swath SAR Imaging", in Pro. EUSAR, pp. 187-192, Hamburg, Germany, June 2016.
- [9] S. Huber, F. Queiroz de Almeida, M. Villano, M. Younis, G. Krieger, A. Moreira, "Tandem-L: A Technical Perspective on Future Spaceborne SAR Sensors for Earth Observation", IEEE Tran. Geosci. and Remote Sen., vol. 56, no. 8, pp. 4792 - 4807, Aug. 2018.
- [10] P. Rosen, S. Hensley, S. Shaffer, W. Edelstein; Y. Kim; R. Kumar; T. Misra; R. Bhan; R. Satish; R. Sagi, "An update on the NASA-ISRO dual-frequency DBF SAR (NISAR) mission", Pro. IGARSS, July 2016.
- [11] G. Krieger, F. Queiroz de Almeida, S. Huber, M. Villano, M. Younis, A. Moreira, et al. "Advanced L-Band SAR System Concepts for High-Resolution Ultra-Wide-Swath SAR Imaging". in ESA Proc. ARSI & KEO, Noordwijk, NL, Sept. 2017.
- [12] F. Bordoni, G. Krieger and M. Younis, "Multifrequency Subpulse SAR: Exploiting Chirp Bandwidth for an Increased Coverage", IEEE Geosci. and Remote Sen. Letters, Vo. 16, No. 1, pp. 40-44, Jan. 2019.
- [13] J. C. Curlander, R. N. McDonough, *Synthetic Aperture Radar: Systems and Signal Processing*, NY, Wiley, 1991.
- [14] F. Bordoni, M. Rodriguez, P. Prats, G. Krieger, "The Effect of Topography on SCORE: an Investigation Based on Simulated Spaceborne Multichannel SAR Data", Pro. EUSAR, pp.1130-4, June 2018.
- [15] M. Younis, T. Rommel, F. Bordoni, G. Krieger, A. Moreira, "On the Pulse Extension Loss in Digital Beamforming SAR", IEEE Geosci. and Remote Sen. Letters, Vol. 12, No. 7, pp. 1436 - 1440, Oct. 2015.